Eur. Phys. J. B **27**, 417–428 (2002)
DOI: 10.1140/epjb/e2002-00173-2

THE EUROPEAN PHYSICAL JOURNAL B

Height and density correlations at liquid surfaces; application to X-ray scattering

S. Mora and J. Daillant[a]

LURE, CNRS-CEA-MINREC, Centre Universitaire Paris-Sud, bâtiment 209D, BP 34, 91898 Orsay Cedex, France
and
Service de Physique de l'État Condensé, CEA Saclay, 91191 Gif-sur-Yvette Cedex, France

Received 12 October 2001
Published online 6 June 2002 –

Abstract. We calculate height-height correlation functions, near-surface density-density correlation functions and the corresponding frequency integrated spectra for a heat conducting viscous fluid. We calculate scattering cross-sections for the static and dynamic X-ray scattering experiments recently developed to investigate the nanometer-scale structure and fluctuations of liquid interfaces. We show that the density-density correlations make an important contribution to the scattering, even using evanescent waves, and that they are strongly affected by the surface. We also discuss the implications for X-ray photon correlation spectroscopy and X-ray inelastic scattering.

PACS. 61.10.-i X-ray diffraction and scattering – 68.03.-g Gas-liquid and vacuum-liquid interfaces – 68.03.Kn Dynamics (capillary waves)

1 Introduction

Although studied for more than a century [1], the structure and dynamics of liquid surfaces still attract considerable interest. Surface excitations have been extensively studied from the 1960's using light scattering [2–9]. In addition to acoustic waves giving rise to Brillouin scattering and non-propagating Rayleigh fluctuations like in the bulk, capillary waves, *i.e.* fluctuations of the interface location itself are characteristic of liquid surfaces. The corresponding spectra were measured by laser light scattering for wavevectors in the range $10^6 - 10^7$ m^{-1} and found in good agreement with theory. X-ray reflectivity [10] and (static) X-ray scattering experiments [11–13] were subsequently applied to liquid surfaces in the late 1980's in order to investigate shorter length scales. Indeed, it proved recently possible to evidence small deviations from the capillary wave spectrum using these techniques [14]. These experiments are very sensitive and the density fluctuations within the 5 nm penetration depth of the evanescent wave used for surface sensitivity make an important contribution to the scattering. Developing a sound basis for the interpretation of these experiments requires the determination of the depth dependence of density fluctuations at the interface and was the first motivation of the present study. Another important motivation is that due to the development of the extremely brilliant so-called third generation synchrotron sources dynamic photon correlation spectroscopy experiments can now be performed on liquid surfaces in the X-ray range [15], and that their interpretation will require the knowledge of all (not only capillary but also density) surface excitation spectra.

For this purpose, we give here a derivation of the height-height and density-density correlation functions at the surface of a viscous, heat-conducting liquid. We follow the method of reference [16] and we use the theory of linear response and the fluctuation-dissipation theorem relating the correlation in fluctuations (here height and density fluctuations) to the response of the system to an external perturbation. The validity of the hydrodynamic approach is guaranteed up to wave vectors $\approx 2 \times 10^9$ m^{-1} by the inelastic scattering measurements of reference [17]. We proceed by determining first the displacement-displacement linear response tensor giving the correlation between the displacements at two different points in the liquid at two different times [18]. Then, we briefly comment on the well-known capillary-wave spectrum, and we discuss in more detail the depth-dependent density fluctuation spectrum, which, to our knowledge, was never given previously. The scattering cross-section for X-rays is determined in a last section.

Water at room temperature is used as an example throughout the paper.

2 The response tensor

Let a variable (here the liquid displacement $\mathbf{u}(\mathbf{r};t)$) of an equilibrium system coupling to a force $\mathbf{F}(\mathbf{r};t)$ through an interaction Hamiltonian $\mathcal{H}$:

$$\mathcal{H} = \int \mathrm{d}\mathbf{r}\, \mathbf{F}(\mathbf{r};t) \cdot \mathbf{u}(\mathbf{r};t)\,. \tag{1}$$

[a] e-mail: daillant@lure.u-psud.fr

Let the response of the system to the applied force being the (ensemble) average liquid displacement at $\mathbf{r}$ and t: $\langle \mathbf{u}(\mathbf{r};t)\rangle$.

The response function $\overline{\overline{\chi}}(\mathbf{r},\mathbf{r}';t)$ is the tensor defined by:

$$\langle \mathbf{u}(\mathbf{r};t)\rangle = \int \mathrm{d}\mathbf{r}' \int_{-\infty}^{t} \mathrm{d}t\, \overline{\overline{\chi}}(\mathbf{r},\mathbf{r}';t-t')\cdot \mathbf{F}(\mathbf{r}';t'). \quad (2)$$

Let us define the displacement-displacement correlation tensor $\overline{\overline{\mathbf{C}}}(\mathbf{r},\mathbf{r}';\tau)$ as: $C_{ij}(\mathbf{r},\mathbf{r}';\tau) = \langle u_i(\mathbf{r};t)u_j(\mathbf{r}';t+\tau)\rangle$, where $i,j \in \{x,y,z\}$. In all what follows, we assume the system to be homogeneous in the plane of the surface ($\mathbf{r}_\parallel$) so that $\overline{\overline{\mathbf{C}}}(\mathbf{r},\mathbf{r}';\tau) = \overline{\overline{\mathbf{C}}}(\mathbf{r}_\parallel - \mathbf{r}'_\parallel, z, z';\tau)$. If we now define the two-dimensional Fourier transform of the displacement $\mathbf{u}\left(\mathbf{q}_\parallel;t\right)$ as

$$\mathbf{u}\left(\mathbf{q}_\parallel,z;t\right) = \lim_{\mathcal{A}\to\infty} \frac{1}{\mathcal{A}} \int_{\mathcal{A}} \mathrm{d}\mathbf{r}_\parallel\, \mathbf{u}(\mathbf{r};\tau)\mathrm{e}^{\mathrm{i}\mathbf{q}_\parallel\cdot\mathbf{r}_\parallel}\,,$$

we have

$$C_{ij}\left(\mathbf{q}_\parallel,z,z';t\right) = \langle u_i(\mathbf{q}_\parallel,z;t)u_j(-\mathbf{q}_\parallel,z';0)\rangle\ \cdot \quad (3)$$

The fluctuation-dissipation theorem relates the correlations in the system to the Fourier transform of the response function (Ref. [19,20]):

$$\overline{\overline{\mathbf{C}}}(\mathbf{r},\mathbf{r}';t) = \frac{k_B T}{\mathrm{i}\pi} \int \mathrm{d}\omega\, \frac{\overline{\overline{\chi}}(\mathbf{r},\mathbf{r}';\omega)}{\omega} \cos(\omega t)\,. \quad (4)$$

A two dimensional Fourier transform (parallel to the plane of the interface xy) followed by simple algebra leads to:

$$\overline{\overline{\mathbf{C}}}\left(\mathbf{q}_\parallel,z,z';\omega\right) = \frac{2k_B T}{\omega} \mathrm{Im}\,\overline{\overline{\chi}}\left(\mathbf{q}_\parallel,z,z';\omega\right) \quad (5)$$

where

$$\overline{\overline{\chi}}\left(\mathbf{q}_\parallel,z,z';\omega\right) = \lim_{\mathcal{A}\to\infty} \frac{1}{\mathcal{A}} \int \mathrm{d}\tau \int_{\mathcal{A}} \mathrm{d}\mathbf{r}_\parallel\, \overline{\overline{\chi}}(\mathbf{r},\mathbf{0};\tau)\mathrm{e}^{\mathrm{i}\left(\omega\tau+\mathbf{q}_\parallel\cdot\mathbf{r}_\parallel\right)}\,,$$

and

$$\overline{\overline{\mathbf{C}}}\left(\mathbf{q}_\parallel,z,z',\omega\right) = \lim_{\mathcal{A}\to\infty} \frac{1}{\mathcal{A}} \int \mathrm{d}\tau \int_{\mathcal{A}} \mathrm{d}\mathbf{r}_\parallel\, \overline{\overline{\mathbf{C}}}(\mathbf{r},\mathbf{0};\tau)\mathrm{e}^{\mathrm{i}\left(\omega\tau+\mathbf{q}_\parallel\cdot\mathbf{r}_\parallel\right)}\,.$$

Using Kramers-Kronig relations and (5), one obtains:

$$\overline{\overline{\mathbf{C}}}\left(\mathbf{q}_\parallel,z,z';\tau=0\right) = k_B T\,\mathrm{Re}\,\overline{\overline{\chi}}\left(\mathbf{q}_\parallel,z,z';\omega=0\right)\,. \quad (6)$$

We will proceed by calculating the displacement in x (parallel to the interface) or z (perpendicular to the interface) produced by an applied force, using the hydrodynamic equations and the appropriate boundary conditions at the surface. We only give a brief outline of the well known hydrodynamic calculations in the next two sections (a complete derivation can be found in reference [21]) and concentrate on the new development, *i.e.* the derivation of all the components of the displacement-displacement response tensor.

2.1 The hydrodynamic equations

The viscous, heat conducting liquid we are considering obeys the continuity equation:

$$\partial\rho/\partial t = -\nabla\cdot(\rho\mathbf{v}), \quad (7)$$

Navier-Stokes equation:

$$\rho\left[(\partial\mathbf{v}/\partial t) + (\mathbf{v}\cdot\nabla)\mathbf{v}\right] - \nabla p - \eta\nabla^2\mathbf{v} - (\zeta + 1/3\eta)\nabla(\nabla\cdot\mathbf{v}) = 0, \quad (8)$$

and the heat conductivity equation:

$$\partial h/\partial t = \kappa\nabla^2 T. \quad (9)$$

$\mathbf{v}$ is the liquid velocity, p is the pressure, and ζ and η are respectively the coefficients of bulk and shear viscosity, $\eta = 1.0019\times10^{-3}\ \mathrm{kg\,m^{-1}\,s^{-1}}$ and $\zeta = 2.1\times10^{-3}\ \mathrm{kg\,m^{-1}\,s^{-1}}$ for water at room temperature [22]. h is the heat density, and κ the thermal conductivity ($0.5925\ \mathrm{W\,m^{-1}\,K^{-1}}$ for water at room temperature). A harmonic time dependence $\exp(-\mathrm{i}\omega t)$ is assumed, leading to $\mathbf{v} = -\mathrm{i}\omega\mathbf{u}$, where $\mathbf{u}$ is the liquid displacement. The thermal excitations we consider are small and it is permissible to linearize the equations, writing for example the total density as $\rho_0+\rho$ where ρ_0 is the constant equilibrium density, and ρ the small fluctuation. After some algebra [21], and using the thermodynamic relations,

$$p = \left(\frac{\partial p}{\partial\rho}\right)_h \rho + \left(\frac{\partial p}{\partial h}\right)_\rho h = \rho v_a^2 + \frac{1}{C_v}\left(\frac{\partial p}{\partial T}\right)_\rho h \quad (10)$$

$$T = \left(\frac{\partial T}{\partial\rho}\right)_h \rho + \left(\frac{\partial T}{\partial h}\right)_\rho h = \frac{T_0}{\rho_0 C_v}\left(\frac{\partial p}{\partial T}\right)_\rho \rho + \frac{h}{C_v} \quad (11)$$

$$\frac{T_0}{\rho_0 C_v}\left(\frac{\partial p}{\partial T}\right)_\rho^2 = \rho_0 v_a^2(1 - C_v/C_p), \quad (12)$$

where v_a is the adiabatic sound velocity, one obtains:

$$\rho = -\rho_0\nabla\cdot\mathbf{u} \quad (13)$$

$$-\rho_0\omega^2\mathbf{u} - \left[\rho_0 v_a^2 - \mathrm{i}\omega(\zeta+4/3\eta)\right]\nabla(\nabla\cdot\mathbf{u}) - \mathrm{i}\omega\eta\nabla\times\nabla\times\mathbf{u}) + \nabla h' = 0 \quad (14)$$

$$-\rho_0 v_a^2\frac{\kappa}{C_p}\left(\frac{C_p}{C_v}-1\right)\nabla^2(\nabla\cdot\mathbf{u}) + \left(\mathrm{i}\omega + \frac{\kappa}{C_v}\nabla^2\right)h' = 0 \quad (15)$$

where $h' = C_v^{-1}(\partial p/\partial T)_\rho h$, and C_v and C_p are the specific heats at constant volume and pressure. $C_p = 4.184\ \mathrm{J\,kg^{-1}\,K^{-1}}$ for water at room temperature, and

using the relationship $C_v = C_p - (TV_{\rm mol}\alpha^2)/\kappa_T$, with $\alpha = 0.2 \times 10^{-3}$ the coefficient of thermal expansion, $V_{\rm mol}$ the molar volume, and $\kappa_T = 4.58 \times 10^{-10}\,{\rm Pa}^{-1}$ the isothermal compressibility, one obtains $C_v = 4.102\ {\rm J\,kg^{-1}\,K^{-1}}$ for water at room temperature.

The equation for the liquid displacement can now be obtained by elimination of h' between (14) and (15). For plane waves $\mathrm{e}^{-\mathrm{i}\mathbf{q}\cdot\mathbf{r}}$,

$$-\rho_0\omega^2\mathbf{u} + \Big[\rho_0 v_a^2 - \mathrm{i}\omega(\zeta + 4/3\eta) + \rho_0 v_a^2 \frac{\kappa}{C_p}(C_p/C_v - 1)\frac{q^2}{\mathrm{i}\omega - \kappa q^2/C_v}\Big] \times \mathbf{q}(\mathbf{q}\cdot\mathbf{u}) + \mathrm{i}\omega\eta\mathbf{q}\times\mathbf{q}\times\mathbf{u} = \mathbf{0}. \quad (16)$$

The solution of this equation in the bulk leads to the existence of two independent transverse modes (shear waves with $\mathbf{q}\cdot\mathbf{u} = 0$) with wavevector q_t such that $q_t^2 = \mathrm{i}\rho_0\omega/\eta \equiv \mathrm{i}\omega/\gamma_t$ and two different longitudinal modes ($\mathbf{q}\times\mathbf{u} = 0$) corresponding to the diffusion of heat with $q_h^2 = \mathrm{i}\omega/\gamma_h = \mathrm{i}\omega C_p/\kappa$ and to damped propagating acoustic waves. The wavevector q_a for the acoustic waves is such that $q_a^2 = \omega^2/(v_a^2 - \mathrm{i}\omega\gamma_a)$ with $\gamma_a = (\zeta + 4/3\eta)/\rho_0 + (\kappa/C_p)(C_p/C_v - 1)$. Another useful quantity is $q_i = \omega^2/(v_i^2 - \mathrm{i}\omega\gamma_i)$ with $v_i^2 = C_v/C_p v_a^2 = (\rho_0\kappa_T)^{-1}$ the isothermal acoustic velocity, and $\gamma_i = (\zeta + 4/3\eta)/\rho_0$.

2.2 Boundary conditions

The hydrodynamic equations must be solved subject to the boundary conditions at the liquid surface $z = 0$ [21]:

$$\big[\rho_0 v_a^2 - \mathrm{i}\omega(\zeta - 2/3\eta)\big]\,\nabla\cdot\mathbf{u} - 2\mathrm{i}\omega\eta\,(\partial u_z/\partial z) - h' = \gamma\left(\partial^2 u_z/\partial z^2\right), \quad (17)$$

$$-\mathrm{i}\omega\eta\,[\partial u_z/\partial x + \partial u_x/\partial z] = 0, \quad (18)$$

$$-\mathrm{i}\omega\eta\,[\partial u_y/\partial z + \partial u_z/\partial y] = 0, \quad (19)$$

$$\partial T/\partial z = 0. \quad (20)$$

The first three equations express the balance of stress at the surface (namely the zz component of the stress tensor is balanced by surface tension, and the xz, and yz components of the stress tensor must be 0), and the last one assumes negligible heat conduction through the surface. γ is the surface tension.

Again equation (20) can be transformed using (11) and h' can be eliminated using equations (17, 20) to obtain equations for the liquid displacement.

2.3 Determination of the response function

In order to obtain the Fourier transform of the response tensor $\overline{\overline{\chi}}$, we calculate the response of the fluid to a force $\mathbf{F}(\mathbf{r};t)$:

$$\mathbf{F}(\mathbf{r};t) = \frac{\mathbf{F_0}}{\mathcal{A}}\exp\left(-\mathrm{i}\omega t - \mathrm{i}\mathbf{q}_\parallel\cdot\mathbf{r}_\parallel\right)\times\delta(z - z') \qquad (z' > 0).$$

Then, (2) leads to:

$$\langle\mathbf{u}\,(\mathbf{r};t)\rangle = \mathrm{e}^{-\mathrm{i}\omega t - \mathrm{i}\mathbf{q}_\parallel\cdot\mathbf{r}_\parallel}\frac{1}{\mathcal{A}}\int_{\mathcal{A}}\mathrm{d}\mathbf{r}''_\parallel\,\overline{\overline{\chi}}(\mathbf{r}_\parallel,\mathbf{r}''_\parallel,z,z';\omega)\mathbf{F_0}\mathrm{e}^{\mathrm{i}\mathbf{q}_\parallel\cdot(\mathbf{r}_\parallel - \mathbf{r}''_\parallel)}\,. \quad (21)$$

and if $\mathcal{A}\to\infty$ one obtains:

$$\langle\mathbf{u}\,(\mathbf{r};t)\rangle = \exp\left(-\mathrm{i}\omega t - \mathrm{i}\mathbf{q}_\parallel\cdot\mathbf{r}_\parallel\right)\overline{\overline{\chi}}(\mathbf{q}_\parallel,z,z';\omega)\cdot\mathbf{F_0}\,.$$

In order to calculate χ_{zz}, we assume that this applied force $\mathbf{F}(\mathbf{r};t)$ is directed parallel to the z axis. Let the x-axis be parallel to $\mathbf{q}_\parallel$ so that the force can be written as:

$$\mathbf{F}(\mathbf{r},t) = \frac{F_0\hat{\mathbf{z}}}{\mathcal{A}}\exp\left(-\mathrm{i}\omega t - \mathrm{i}q_\parallel x\right)\times\delta(z - z')\,.$$

This force couples to a liquid displacement $\mathbf{u}(z)\exp(-\mathrm{i}\omega t - \mathrm{i}q_\parallel x)$ with an interaction Hamiltonian $\mathcal{H} = u_z^*(z')F$. The solution of equations (13–15) in presence of the force is the sum of a particular solution obtained with the force substituted in the second hand of (14) plus a general solution of the free equations adjusted to meet the boundary conditions. From $u_z(z)$, one obtains the zz component of the response function tensor:

$$\chi_{zz}(\mathbf{q}_\parallel,z,z';\omega) = \langle u_z(z)\rangle/F_0. \quad (22)$$

According to reference [21]:

$$\begin{aligned}\chi_{zz}(\mathbf{q}_\parallel,z,z';\omega) &= \frac{\mathrm{i}}{2\rho_0\mathcal{A}\omega^2}\\ &\times\Bigg\langle\frac{q_\parallel^2}{q_t^z}\mathrm{e}^{\mathrm{i}q_t^z|z-z'|} + \frac{q_i^2 - q_a^2}{q_h^2 - q_a^2}q_h^z\mathrm{e}^{\mathrm{i}q_h^z|z-z'|} + \frac{q_h^2 - q_i^2}{q_h^2 - q_a^2}q_a^z\mathrm{e}^{\mathrm{i}q_a^z|z-z'|}\\ &- \Bigg\{D(+--)\frac{q_\parallel^2}{q_t^z}\mathrm{e}^{-\mathrm{i}q_t^z z'} - 2Cq_\parallel^2\Big[(q_i^2 - q_a^2)\mathrm{e}^{-\mathrm{i}q_h^z z'}\\ &\quad + (q_h^2 - q_i^2)\mathrm{e}^{-\mathrm{i}q_a^z z'}\Big]\Bigg\}\times\frac{\mathrm{e}^{-\mathrm{i}q_t^z z}}{D(+++)}\\ &+\Bigg\{(q_i^2 - q_a^2)C\left[2q_\parallel^2\mathrm{e}^{-\mathrm{i}q_t^z z'} + \frac{q_h^2 - q_i^2}{q_h^2 - q_a^2}(q_t^2 - 2q_\parallel^2)\mathrm{e}^{-\mathrm{i}q_a^z z'}\right]\\ &\quad - D(-++)\frac{q_i^2 - q_a^2}{q_h^2 - q_a^2}q_h^z\mathrm{e}^{-\mathrm{i}q_h^z z'}\Bigg\}\frac{\mathrm{e}^{-\mathrm{i}q_h^z z}}{D(+++)}\\ &+\Bigg\{(q_h^2 - q_i^2)C\left[2q_\parallel^2\mathrm{e}^{-\mathrm{i}q_t^z z'} + \frac{q_i^2 - q_a^2}{q_h^2 - q_a^2}(q_t^2 - 2q_\parallel^2)\mathrm{e}^{-\mathrm{i}q_h^z z'}\right]\\ &\quad + D(--+)\frac{q_h^2 - q_i^2}{q_h^2 - q_a^2}q_a^z\mathrm{e}^{-\mathrm{i}q_a^z z'}\Bigg\}\frac{\mathrm{e}^{-\mathrm{i}q_a^z z}}{D(+++)}\Bigg\rangle, \quad (23)\end{aligned}$$

$$\chi_{xz}(\mathbf{q}_\parallel,z,z';\omega)=\frac{\mathrm{i}}{2\rho_0\mathcal{A}\omega^2}\times\Bigg\langle -q_\parallel\left[-\mathrm{e}^{\mathrm{i}q_t^z|z-z'|}+\frac{q_i^2-q_a^2}{q_h^2-q_a^2}\mathrm{e}^{\mathrm{i}q_h^z|z-z'|}+\frac{q_h^2-q_i^2}{q_h^2-q_a^2}\mathrm{e}^{\mathrm{i}q_a^z|z-z'|}\right]\mathrm{sgn}(z-z')$$
$$+\left\{D(+--)q_\parallel\mathrm{e}^{-\mathrm{i}q_t^z z'}-2Cq_\parallel q_z^t\left[(q_i^2-q_a^2)\mathrm{e}^{-\mathrm{i}q_h^z z'}+(q_h^2-q_i^2)\mathrm{e}^{-\mathrm{i}q_a^z z'}\right]\right\}$$
$$\times\frac{\mathrm{e}^{-\mathrm{i}q_t^z z}}{D(+++)}$$
$$+\left\{(q_i^2-q_a^2)C\frac{q_\parallel}{q_h^z}\left[2q_\parallel^2\mathrm{e}^{-\mathrm{i}q_t^z z'}+\frac{q_h^2-q_i^2}{q_h^2-q_a^2}(q_t^2-2q_\parallel^2)\mathrm{e}^{-\mathrm{i}q_a^z z'}\right]\right.$$
$$\left.+D(-++)\frac{q_i^2-q_a^2}{q_h^2-q_a^2}q_\parallel\mathrm{e}^{-\mathrm{i}q_h^z z'}\right\}\frac{\mathrm{e}^{-\mathrm{i}q_h^z z}}{D(+++)}$$
$$+\left\{(q_h^2-q_i^2)C\frac{q_\parallel}{q_a^z}\left[2q_\parallel^2\mathrm{e}^{-\mathrm{i}q_t^z z'}+\frac{q_i^2-q_a^2}{q_h^2-q_a^2}(q_t^2-2q_\parallel^2)\mathrm{e}^{-\mathrm{i}q_h^z z'}\right]\right.$$
$$\left.-D(--+)\frac{q_h^2-q_i^2}{q_h^2-q_a^2}q_\parallel\mathrm{e}^{-\mathrm{i}q_a^z z'}\right\}\frac{\mathrm{e}^{-\mathrm{i}q_a^z z}}{D(+++)}\Bigg\rangle. \tag{26}$$

$$\chi_{zx}(\mathbf{q}_\parallel,z,z';\omega)=\frac{\mathrm{i}}{2\rho_0\mathcal{A}\omega^2}\times\Bigg\langle -q_\parallel\left[-\mathrm{e}^{\mathrm{i}q_t^z|z-z'|}+\frac{q_i^2-q_a^2}{q_h^2-q_a^2}\mathrm{e}^{\mathrm{i}q_h^z|z-z'|}+\frac{q_h^2-q_i^2}{q_h^2-q_a^2}\mathrm{e}^{\mathrm{i}q_a^z|z-z'|}\right]\mathrm{sgn}(z-z')$$
$$+\left\{-D(+--)q_\parallel\mathrm{e}^{-\mathrm{i}q_t^z z'}+2Cq_\parallel^2\left[\frac{q_\parallel}{q_h^z}(q_i^2-q_a^2)\mathrm{e}^{-\mathrm{i}q_h^z z'}+\frac{q_\parallel}{q_a^z}(q_h^2-q_i^2)\mathrm{e}^{-\mathrm{i}q_a^z z'}\right]\right\}$$
$$\times\frac{\mathrm{e}^{-\mathrm{i}q_t^z z}}{D(+++)}$$
$$-\left\{(q_i^2-q_a^2)C\left[-2q_\parallel q_t^z\mathrm{e}^{-\mathrm{i}q_t^z z'}+\frac{q_h^2-q_i^2}{q_h^2-q_a^2}(q_t^2-2q_\parallel^2)\frac{q_\parallel}{q_a^z}\mathrm{e}^{-\mathrm{i}q_a^z z'}\right]\right.$$
$$\left.-D(-++)\frac{q_i^2-q_a^2}{q_h^2-q_a^2}q_\parallel\mathrm{e}^{-\mathrm{i}q_h^z z'}\right\}\frac{\mathrm{e}^{-\mathrm{i}q_h^z z}}{D(+++)}$$
$$-\left\{(q_h^2-q_i^2)C\left[-2q_\parallel q_t^z\mathrm{e}^{-\mathrm{i}q_t^z z'}+\frac{q_i^2-q_a^2}{q_h^2-q_a^2}(q_t^2-2q_\parallel^2)\frac{q_\parallel}{q_h^z}\mathrm{e}^{-\mathrm{i}q_h^z z'}\right]\right.$$
$$\left.+D(--+)\frac{q_h^2-q_i^2}{q_h^2-q_a^2}q_\parallel\mathrm{e}^{-\mathrm{i}q_a^z z'}\right\}\frac{\mathrm{e}^{-\mathrm{i}q_a^z z}}{D(+++)}\Bigg\rangle. \tag{27}$$

with

$$D(\pm\pm\pm)=\left[\left(q_h^2-q_i^2\right)q_h^z\pm\left(q_i^2-q_a^2\right)q_a^z\right]\left(q_t^2-2q_\parallel^2\right)^2\rho_0\omega^2$$
$$\pm\left(q_h^2-q_a^2\right)q_h^zq_a^zq_\parallel^2\left(4\rho_0\omega^2q_t^z\pm\mathrm{i}\gamma q_t^4\right) \tag{24}$$

$$C=2\rho_0\omega^2q_h^zq_a^z(q_t^2-2q_\parallel^2). \tag{25}$$

The terms in $|z-z'|$ are bulk solutions of the hydrodynamic equations for respectively the transerve waves, longitudinal fluctuations related to the diffusion of heat, and longitudinal acoustic waves. The other terms include reflections at the surface and allow the fullfilement of the boundary conditions.

$\chi_{xz}(\mathbf{q}_\parallel,z,z';\omega)$ can be deduced from $\chi_{zz}(\mathbf{q}_\parallel,z,z';\omega)$ as follows. $\chi_{xz}(\mathbf{q}_\parallel,z,z';\omega)$ is obtained from the x displacement due to the same vertical force. Let's for example first consider the transverse $\exp(\mathrm{i}q_t^z|z-z'|-\mathrm{i}q_\parallel x)$ bulk wave. It can be rewritten $\exp(\mathrm{i}q_t^z(z-z')\mathrm{sgn}(z-z')-\mathrm{i}q_\parallel x)$. Since it is a transverse wave, $\mathbf{q}\cdot\mathbf{u}=0$; hence $q_t^z\mathrm{sgn}(z-z')u_z-q_\parallel u_x=0$, and the x displacement is obtained by multiplying the z displacement by $q_t^z/q_\parallel\times\mathrm{sgn}(z-z')$. Applying the same reasoning, longitudinal bulk waves for which $\mathbf{q}\times\mathbf{u}=0$ must be multiplied by $-q_\parallel/q^z\times\mathrm{sgn}(z-z')$, transverse $(z+z')$ waves by $-q_t^z/q_\parallel$, and longitudinal $(z+z')$ waves by $q_\parallel/q^z$. Using these symmetry properties, one obtains.

See equation (26) above.

$\chi_{zx}(\mathbf{q}_\parallel,z,z';\omega)$ is the z displacement response to an horizontal applied force, and cannot therefore be obtained using the same method. We now use the general symmetry property $\chi_{ij}(\mathbf{r},\mathbf{r}';\omega)=\chi_{ji}(\mathbf{r}',\mathbf{r};\omega)$ [19,23] which implies $\chi_{zx}(\mathbf{q}_\parallel,z,z';\omega)=\chi_{xz}(-\mathbf{q}_\parallel,z,z';\omega)$:

See equation (27) above.

We finally get $\chi_{xx}(\mathbf{q}_\parallel,z,z';\omega)$ by multiplying transverse bulk waves $-q_t^z/q_\parallel\times\mathrm{sgn}(z-z')$, longitudinal bulk waves by $q_\parallel/q^z\times\mathrm{sgn}(z-z')$, transverse $(z+z')$ waves by $q_t^z/q_\parallel$, and longitudinal $(z+z')$ waves by $-q_\parallel/q^z$.

See equation (28) next page.

We now have derived all the response tensor components we need to determine height or density correlation functions. We start by briefly discussing the well-known height-height correlation function.

$$\chi_{xx}(\mathbf{q}_\parallel, z, z'; \omega) = \frac{\mathrm{i}}{2\rho_0 \mathcal{A}\omega^2} \times \left\langle \left[q_t^z \mathrm{e}^{\mathrm{i}q_t^z|z-z'|} + \frac{q_i^2 - q_a^2}{q_h^2 - q_a^2} \frac{q_\parallel^2}{q_h^z} \mathrm{e}^{\mathrm{i}q_h^z|z-z'|} + \frac{q_h^2 - q_i^2}{q_h^2 - q_a^2} \frac{q_\parallel^2}{q_a^z} \mathrm{e}^{\mathrm{i}q_a^z|z-z'|} \right] \right.$$
$$+ \left\{ D(+--) q_t^z \mathrm{e}^{-\mathrm{i}q_t^z z'} + 2Cq_\parallel^2 \left[\frac{q_t^z}{q_h^z}(q_i^2 - q_a^2)\mathrm{e}^{-\mathrm{i}q_h^z z'} + \frac{q_t^z}{q_a^z}(q_h^2 - q_i^2)\mathrm{e}^{-\mathrm{i}q_a^z z'} \right] \right\}$$
$$\times \frac{\mathrm{e}^{-\mathrm{i}q_t^z z}}{D(+++)}$$
$$- \left\{ (q_i^2 - q_a^2) C \frac{q_\parallel}{q_h^z} \left[-2q_\parallel q_t^z \mathrm{e}^{-\mathrm{i}q_t^z z'} + \frac{q_h^2 - q_i^2}{q_h^2 - q_a^2}(q_t^2 - 2q_\parallel^2) \frac{q_\parallel}{q_a^z} \mathrm{e}^{-\mathrm{i}q_a^z z'} \right] \right.$$
$$\left. - D(-++) \frac{q_i^2 - q_a^2}{q_h^2 - q_a^2} \frac{q_\parallel^2}{q_h^z} \mathrm{e}^{-\mathrm{i}q_h^z z'} \right\} \frac{\mathrm{e}^{-\mathrm{i}q_h^z z}}{D(+++)}$$
$$- \left\{ (q_h^2 - q_i^2) C \frac{q_\parallel}{q_a^z} \left[-2q_\parallel q_t^z \mathrm{e}^{-\mathrm{i}q_t^z z'} + \frac{q_i^2 - q_a^2}{q_h^2 - q_a^2}(q_t^2 - 2q_\parallel^2) \frac{q_\parallel}{q_h^z} \mathrm{e}^{-\mathrm{i}q_h^z z'} \right] \right.$$
$$\left. + D(--+) \frac{q_h^2 - q_i^2}{q_h^2 - q_a^2} \frac{q_\parallel^2}{q_a^z} \mathrm{e}^{-\mathrm{i}q_a^z z'} \right\} \frac{\mathrm{e}^{-\mathrm{i}q_a^z z}}{D(+++)} \left. \right\rangle . \tag{28}$$

$$C_{zz}(\mathbf{q}_\parallel, 0, 0; \omega) = \frac{2k_B T}{\mathcal{A}\omega} \mathrm{Re} \left(\frac{1}{\left[\left(\frac{q_h^2 - q_i^2}{q_h^2 - q_a^2} \frac{1}{q_a^z} + \frac{q_i^2 - q_a^2}{q_h^2 - q_a^2} \frac{1}{q_h^z} \right) \left(1 - \frac{2q_\parallel^2}{q_t^2} \right)^2 \rho_0 \omega^2 + q_\parallel^2 \left(\frac{4\rho_0 \omega^2 q_t^z}{q_t^4} + \mathrm{i}\gamma \right) \right]} \right), \tag{30}$$

3 The surface height-height correlation function

The surface height-height correlation function is simply the displacement-displacement correlation function for $z = z' = 0$. Using equation (23), and grouping the different terms for $z = z' = 0$, one obtains:

$$\chi_{zz}(\mathbf{q}_\parallel, 0, 0; \omega) = \frac{\mathrm{i}}{\mathcal{A}} \frac{(q_h^2 - q_a^2) q_h^z q_a^z q_t^4}{D(+++)} \cdot \tag{29}$$

The fluctuation-dissipation theorem equation (5) yields:

See equation (30) above,

which is the height-height fluctuation spectrum. This spectrum shows two peaks in the region of capillary wave frequency and in the region of acoustic wave frequency (Fig. 1a). All the simulations presented in this paper are for water at room temperature, where we used the numerical values of Table 1. For small viscosities, equation (30) can be approximated in the capillary-wave region as a Lorentzian with half-width at half-maximum $2\eta q_\parallel^2/\rho_0$, which is the damping term for capillary waves [16]. The other peak corresponds to bulk acoustic waves propagating parallel to the surface. Its dispersion relation is $\omega = v_a q$, whereas the dispersion relation of capillary waves is $\omega^2 = \gamma/\rho_0 q^3$. We note in Figure 1a that there is no peak in the capillary waves spectrum for $q_\parallel > 10^8$ m^{-1} and in the acoustic wave spectrum at 10^9 m^{-1}. This means that capillary waves are overdamped for $q_\parallel > 10^8$ m^{-1} and that acoustic waves are overdamped at 10^9 m^{-1}. This will also

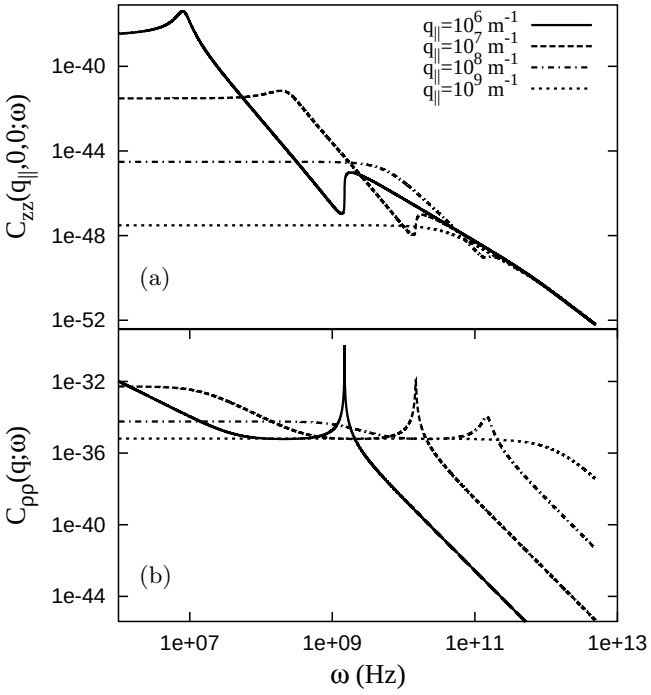

Fig. 1. (a) Capillary wave spectra for $q_\parallel = 10^6$ m^{-1}, 10^7 m^{-1}, 10^8 m^{-1}, and 10^9 m^{-1} respectively. Note the capillary wave peak and the higher frequency surface acoustic wave peak. Capillary waves are overdamped for $q_\parallel > 10^8$ m^{-1} and acoustic waves at 10^9 m^{-1}. The area under the curve decreases as $k_B T/\gamma {q_\parallel}^2$. (b) Bulk density fluctuation spectra for $q = 10^6$ m^{-1}, 10^7 m^{-1}, 10^8 m^{-1}, and 10^9 m^{-1} respectively. Note the zero-frequency peak associated with thermal diffusion and the propagating acoustic wave peak.

Table 1. Numerical values of the thermodynamical and hydrodynamical parameters of water at room temperature used for the simulations presented in this paper.

ρ_0	γ	η	ζ	κ	v_a	C_p	C_v
$\mathrm{kg\,m^{-3}}$	$\mathrm{N/m}$	$\mathrm{kg\,m^{-1}\,s^{-1}}$	$\mathrm{kg\,m^{-1}\,s^{-1}}$	$\mathrm{W\,m^{-1}\,K^{-1}}$	$\mathrm{m\,s^{-1}}$	$\mathrm{J\,m^{-3}\,K^{-1}}$	$\mathrm{J\,m^{-3}\,K^{-1}}$
10^3	72.8×10^{-3}	1.0019×10^{-3}	2.1×10^{-3}	0.5925	1.482×10^3	4.184×10^6	4.102×10^6

appear in Figure 3 below, where the oscillatory behaviour at wave-vectors smaller than 10^8 m^{-1} and the damping at 10^8 m^{-1} are explicitly shown. The damping constant for overdamped waves, $\gamma q_\parallel/\eta$, can again be obtained by approximating equation (30) [16].

The question of the contribution of overdamped capillary waves to the surface roughness has been recently addressed [24]. The answer given to this question by the fluctuation-dissipation theorem is unambiguous: Substituting equation (29) in equation (6) and going to the limit $\omega \to 0$, one obtains the integrated spectrum,

$$\left\langle |u_z\left(\mathbf{q}_\parallel, 0, 0; t=0\right)|^2 \right\rangle = \frac{k_B T}{\mathcal{A}\gamma q_\parallel^2}\cdot \tag{31}$$

Equation (29) gives the integrated spectrum whatever the viscosity or even the nature of the fluctuations (non-propagating, capillary or acoustic). In other words, *at equilibrium*, only the free energy cost of deforming the surface which is given by the increase in area multiplied by surface tension is important in determining the integrated height-height correlations, as expected.

4 The near-surface density-density correlation function

4.1 The response function

The linear response function for density fluctuations is obtained by derivation of the displacement-displacement response tensor.

Let us define the potential $V(\mathbf{r},t)$ such that $\mathbf{F}(\mathbf{r},t) = -\nabla V(\mathbf{r},t)$. Then, using $\rho = -\rho_0 \nabla.\mathbf{u}$ (13), and integrating by parts, equation (1) leads to:

$$\begin{aligned}\mathcal{H} &= \int \mathbf{F}(\mathbf{r};t).\mathbf{u}(\mathbf{r};t)\,\mathrm{d}\mathbf{r} = -\int \nabla V(\mathbf{r};t).\mathbf{u}(\mathbf{r};t)\,\mathrm{d}\mathbf{r}\\ &= \frac{1}{\rho_0}\int \rho(\mathbf{r};t)V(\mathbf{r};t)\,\mathrm{d}\mathbf{r}\end{aligned}$$

which shows that $V(\mathbf{r};t)$ is the potential coupled with density, and the density response function $\chi_{\rho\rho}(\mathbf{r},\mathbf{r}';t-t')$ can be defined as

$$\langle\rho(\mathbf{r};t)\rangle = \int \mathrm{d}\mathbf{r}' \int_{-\infty}^{t} \mathrm{d}t\; \chi_{\rho\rho}(\mathbf{r},\mathbf{r}';t-t')V(\mathbf{r}';t'). \tag{32}$$

Using again (13), we have

$$\begin{aligned}\langle\rho(\mathbf{r};t)\rangle &= -\rho_0\langle\nabla\cdot\mathbf{u}(\mathbf{r};t)\rangle\\ &= -\rho_0\int \mathrm{d}\mathbf{r}'\int_{-\infty}^{t}\mathrm{d}t\;\nabla\cdot\left[\overline{\overline{\chi}}(\mathbf{r},\mathbf{r}';t-t')\cdot\mathbf{F}(\mathbf{r}';t')\right],\end{aligned} \tag{33}$$

leading after integration by parts to

$$\begin{aligned}\langle\rho(\mathbf{r};t)\rangle = \rho_0\int \mathrm{d}\mathbf{r}'\Bigg[&\frac{\partial^2\chi_{xx}(\mathbf{r},\mathbf{r}';t)}{\partial x\partial x'} + \frac{\partial^2\chi_{zx}(\mathbf{r},\mathbf{r}';t)}{\partial z\partial x'}\\ &+\frac{\partial^2\chi_{xz}(\mathbf{r},\mathbf{r}';t)}{\partial x\partial z'} + \frac{\partial^2\chi_{zz}(\mathbf{r},\mathbf{r}';t)}{\partial z\partial z'}\Bigg]\; V(\mathbf{r}';t),\end{aligned} \tag{34}$$

and the density-density response function is:

$$\begin{aligned}\chi_{\rho\rho}(\mathbf{q}_\parallel,z,z';\omega) = \rho_0^2\Bigg(&\frac{\partial^2\chi_{xx}(\mathbf{r},\mathbf{r}';\omega)}{\partial x\partial x'} + \frac{\partial^2\chi_{zx}(\mathbf{r},\mathbf{r}';\omega)}{\partial z\partial x'}\\ &+\frac{\partial^2\chi_{xz}(\mathbf{r},\mathbf{r}';\omega)}{\partial x\partial z'} + \frac{\partial^2\chi_{zz}(\mathbf{r},\mathbf{r}';\omega)}{\partial z\partial z'}\Bigg).\end{aligned} \tag{35}$$

One obtains:

$$\begin{aligned}\chi_{\rho\rho}(\mathbf{q}_\parallel,z,z';\omega) = \frac{\mathrm{i}\rho_0}{2\omega^2}\times\Bigg\{&\left[\frac{q_i^2-q_a^2}{q_h^2-q_a^2}\frac{q_h^4}{q_h^z}\mathrm{e}^{\mathrm{i}q_h^z|z-z'|}\right.\\ &\left.+\frac{q_h^2-q_i^2}{q_h^2-q_a^2}\frac{q_a^4}{q_a^z}\mathrm{e}^{\mathrm{i}q_a^z|z-z'|} - 2\mathrm{i}q_i^2\delta(z-z')\right]\\ &-\left[(q_i^2-q_a^2)C\frac{q_h^2-q_i^2}{q_h^2-q_a^2}(q_t^2-2q_\parallel^2)\frac{q_h^2q_a^2}{q_h^zq_a^z}\mathrm{e}^{-\mathrm{i}q_a^zz'}\right.\\ &\left.-D(-++)\frac{q_i^2-q_a^2}{q_h^2-q_a^2}\frac{q_h^4}{q_h^z}\mathrm{e}^{-\mathrm{i}q_h^zz'}\right]\frac{\mathrm{e}^{-\mathrm{i}q_h^zz}}{D(+++)}\\ &-\left[(q_h^2-q_i^2)C\frac{q_i^2-q_a^2}{q_h^2-q_a^2}(q_t^2-2q_\parallel^2)\frac{q_h^2q_a^2}{q_h^zq_a^z}\mathrm{e}^{-\mathrm{i}q_h^zz'}\right.\\ &\left.+D(--+)\frac{q_h^2-q_i^2}{q_h^2-q_a^2}\frac{q_a^4}{q_a^z}\mathrm{e}^{-\mathrm{i}q_a^zz'}\right]\frac{\mathrm{e}^{-\mathrm{i}q_a^zz}}{D(+++)}\Bigg\}.\end{aligned} \tag{36}$$

As expected, transverse waves do not appear in this density-density response function. An interesting point is the influence of the depth dependence of the correlation function on X-ray scattering experiments. We will discuss this in the next section after establishing the expression of the scattering cross-section. Before this, we briefly recall the characteristics of the bulk density-density correlation function.

4.2 Determination of the density-density correlation function

The density-density correlation function is obtained from equation (36) by applying the fluctuation dissipation theorem equation (5):

$$C_{\rho\rho}(\mathbf{q}_\parallel,z,z';\omega) = \frac{2k_BT}{\omega}\,\mathrm{Im}\chi_{\rho\rho}(\mathbf{q}_\parallel,z,z';\omega)\,, \tag{37}$$

with $C_{\rho\rho}(\mathbf{r},\mathbf{r}';t) = \langle\rho(\mathbf{r},0)\rho(\mathbf{r}',t)\rangle$.

The first term between square brackets in (36) which correspond to the bulk excitations leads after Fourier transformation (including in the vertical z-direction) and grouping of the terms to:

$$C_{\rho\rho}(\mathbf{q};\omega) = \frac{2\rho_0\, k_B T}{\omega^3 V} \frac{q^2(q_i^2 q^2 - q_a^2 q_h^2)}{(q^2 - q_h^2)(q^2 - q_a^2)}\,. \tag{38}$$

This spectrum is composed of two outer peaks associated with propagating acoustic waves and giving rise to Brillouin scattering, and of a central peak associated with thermal diffusion and giving rise to Rayleigh scattering (Fig. 1b). The ratio of the integrated contributions $(C_p/C_v) - 1$ is the Landau-Placzek ratio.

The integrated spectrum can be easily calculated using Kramers-Kronig relations equation (6):

$$C_{\rho\rho}(\mathbf{q}_\parallel, z, z'; t = 0) = k_B T\, \mathrm{Re}\chi_{\rho\rho}(\mathbf{q}_\parallel, z, z'; \omega = 0)\,. \tag{39}$$

In the limit $\omega \to 0$, the only non-vanishing term in equation (36) is the third one, whose limit is $\rho_0/v_i^2 \times \delta(z - z')$. From equation (39), one obtains:

$$C_{\rho\rho}(\mathbf{q}_\parallel, z, z'; t = 0) = \frac{\rho_0^2\, k_B T \kappa_T}{\mathcal{A}}\, \delta(z - z'). \tag{40}$$

Equation (40) is the well-known result that density-density fluctuations are proportional to the isothermal compressibility of the fluid. In the bulk,

$$C_{\rho\rho}(\mathbf{q}; t = 0) = \frac{\rho_0^2\, k_B T \kappa_T}{V}, \tag{41}$$

where V is the volume considered.

5 Scattering cross-section for X-rays

5.1 Scattering cross-section for X-rays within the distorted-wave Born approximation

The interpretation of a diffraction or diffuse scattering experiment generally requires the comparison of an experimentally determined scattered intensity with a model calculation. This is most conveniently achieved by calculating the differential scattering cross-section $\mathrm{d}\sigma/\mathrm{d}\Omega$ which is defined as the intensity scattered per unit solid angle in the direction $\mathbf{k}_{\mathrm{sc}}$ for a unit incident flux in the direction $\mathbf{k}_{\mathrm{in}}$. The scattered intensity is then obtained by convoluting $\mathrm{d}\sigma/\mathrm{d}\Omega$ with the experimental resolution function.

As long as the frequency of the electromagnetic field is much larger than the characteristic atomic frequencies, which is the case for the generally light atoms considered in soft-condensed matter, the electrons can be considered as free electrons [25], and a material can be simply characterised by its electron density ρ_e. More precisely, for waves with a $\mathrm{e}^{\mathrm{i}\omega t}$ time dependence, the optical index can be written:

$$n = 1 - \delta - \mathrm{i}\beta; \quad \text{with} \quad \delta = \frac{\lambda^2}{2\pi} r_e \rho_e, \tag{42}$$

where λ is electromagnetic wave length, and $r_e = 2.818 \times 10^{-15}$ m is the so-called classical electron radius, which is the scattering length for Thomson scattering. In the most simple Born approximation (kinematic approximation) which neglects multiple scattering, a given electron only "sees" the incident wave, and the waves scattered by two electrons separated by a distance $\mathbf{r}$ only differ by a phase factor $\mathrm{e}^{\mathrm{i}\mathbf{q}\cdot\mathbf{r}}$, where $\mathbf{q} = \mathbf{k}_{\mathrm{sc}} - \mathbf{k}_{\mathrm{in}}$ is the wave-vector transfer. Summing over all electrons in the medium and going to the continuous limit, we have for the scattering cross-section:

$$\mathrm{d}\sigma/\mathrm{d}\Omega = r_e^2 \left| \int \mathrm{d}\mathbf{r} \rho_e(\mathbf{r}) \mathrm{e}^{\mathrm{i}\mathbf{q}\cdot\mathbf{r}} \right|^2, \tag{43}$$

where the electron density can be written as the convolution of the atomic or molecular density $\sum_i \delta(\mathbf{r} - \mathbf{r}_i)$ with the electron distribution $f(\mathbf{r})$ in the atom or molecule:

$$\rho_e(\mathbf{r}) = \sum_i \delta(\mathbf{r} - \mathbf{r}_i) \otimes f(\mathbf{r}). \tag{44}$$

The Fourier transform of $f(\mathbf{r})$ is the atomic or molecular form factor $f(\mathbf{q})$ which for small enough wave vectors is simply equal to the number of electrons in the atom or molecule. We will use this approximation in the following, which allows us to simply replace ρ_0 by the average electron density ρ_e in equations (36–41) to calculate electron density correlations.

In fact, the Born approximation is generally not accurate enough, and this is in particular the case for surfaces, as can be easily seen using equation (42). Indeed, since the refractive index of matter is (slightly) less than 1, it is straightforward to show using the Snell-Descartes law of refraction that total external reflection occurs for grazing angles of incidence $\theta_{\mathrm{in}} \leq \theta_c = \sqrt{2\delta} \approx 10^{-3}$. This phenomenon is of great help for the study of surfaces since for $\theta_{\mathrm{in}} < \theta_c$ only an evanescent wave propagates below the surface (with a penetration depth equal to a few nm), and hence surface sensitivity is considerably enhanced. On the other hand, scattering cross-sections are large in the total external reflection region, multiple scattering cannot be neglected, and the simple kinematical approach presented above is no longer good enough. More accurate methods are to be used, the most popular being the distorted-wave Born approximation (DWBA). Within this approximation, the scattering cross-section is now [26,27]:

$$\mathrm{d}\sigma/\mathrm{d}\Omega = \mathrm{d}\sigma/\mathrm{d}\Omega_{\mathrm{ref}} + r_e^2 \left|t_{0,1}^{\mathrm{in}}\right|^2 \left|t_{0,1}^{\mathrm{sc}}\right|^2 \times (\widehat{\mathbf{e}}_{\mathrm{in}} \cdot \widehat{\mathbf{e}}_{\mathrm{sc}})^2 \left\langle \left| \int \mathrm{d}\mathbf{r} \delta\rho_e(\mathbf{r}) \mathrm{e}^{\mathrm{i}\mathbf{q}\cdot\mathbf{r}} \right|^2 \right\rangle, \tag{45}$$

where $\mathrm{d}\sigma/\mathrm{d}\Omega_{\mathrm{ref}}$ is the scattering cross section for specular reflection from the perfect interface without fluctuations. $\delta\rho_e(\mathbf{r})$ is the difference between the actual electron density and that of the perfect dioptre. $t_{0,1}^{\mathrm{in}}$ and $t_{0,1}^{\mathrm{sc}}$ are the Fresnel transmission coefficients between the upper (0) and lower (1) media, for respectively the angle of incidence θ_{in} and the scattering angle in the scattering plane θ_{sc}. The coefficient $t_{0,1}^{\mathrm{in}}$ is an approximation of the actual field scattered by the electron density fluctuations, and $t_{0,1}^{\mathrm{sc}}$ describes how this field propagates to the detector. $(\widehat{\mathbf{e}}_{\mathrm{in}} \cdot \widehat{\mathbf{e}}_{\mathrm{sc}})^2$ is a polarisation factor not considered in equation (43) obtained for scalar waves. $\widehat{\mathbf{e}}_{\mathrm{in}}$ is the polarisation vector of the incident field, and $\widehat{\mathbf{e}}_{\mathrm{sc}}$ that of the scattered field.

5.2 Integrated spectra

Starting from equation (45), we obtain:

$$\begin{aligned}\mathrm{d}\sigma/\mathrm{d}\Omega = {} & \mathrm{d}\sigma/\mathrm{d}\Omega_{\mathrm{ref}} \\ & + r_e^2 \left|t_{0,1}^{\mathrm{in}}\right|^2 \left|t_{0,1}^{\mathrm{sc}}\right|^2 (\widehat{\mathbf{e}}_{\mathrm{in}}.\widehat{\mathbf{e}}_{\mathrm{sc}})^2 \int \mathrm{d}\mathbf{r} \int \mathrm{d}\mathbf{r}' \mathrm{e}^{\mathrm{i}\mathbf{q}_\parallel \cdot (\mathbf{r}_\parallel - \mathbf{r}'_\parallel)} \\ & \ldots \left\langle \int_{-\infty}^{u_z(\mathbf{r}_\parallel,0)} \mathrm{d}z \int_{-\infty}^{u_z(\mathbf{r}'_\parallel,0)} \mathrm{d}z' \delta\rho_e(\mathbf{r}_\parallel, z) \right. \\ & \left. \times \delta\rho_e^*(\mathbf{r}'_\parallel, z') \mathrm{e}^{\mathrm{i}(q_z z - q_z^* z')} \right\rangle . \quad (46)\end{aligned}$$

In fact, at the liquid surface, $\delta\rho_e$ can be of two different origins: there are usual density fluctuations $\delta\rho_{\mathrm{dens}}$ calculated above, and there also are places where liquid (resp. vapour) in the perfect dioptre has been replaced by vapour (resp. liquid) due to interface fluctuations. After some algebra, we obtain [27]:

$$\begin{aligned}\mathrm{d}\sigma/\mathrm{d}\Omega = {} & \mathrm{d}\sigma/\mathrm{d}\Omega_{\mathrm{ref}} + r_e^2 \left|t_{0,1}^{\mathrm{in}}\right|^2 \left|t_{0,1}^{\mathrm{sc}}\right|^2 (\widehat{\mathbf{e}}_{\mathrm{in}}.\widehat{\mathbf{e}}_{\mathrm{sc}})^2 \\ & \times \int \mathrm{d}\mathbf{r} \int \mathrm{d}\mathbf{r}' \mathrm{e}^{\mathrm{i}\mathbf{q}_\parallel \cdot (\mathbf{r}_\parallel - \mathbf{r}'_\parallel)} \left[\left\langle \int_{-\infty}^{u_z(\mathbf{r}_\parallel,0)} \mathrm{d}z \int_{-\infty}^{u_z(\mathbf{r}'_\parallel,0)} \mathrm{d}z' \right. \right. \\ & \left. \times \delta\rho_{\mathrm{dens}}(\mathbf{r}_\parallel, z) \delta\rho_{\mathrm{dens}}^*(\mathbf{r}'_\parallel, z') \mathrm{e}^{\mathrm{i}(q_z z - q_z^* z')} \right\rangle \\ & \left. + \rho_{\mathrm{sub}}^2 \left\langle \int_0^{u_z(\mathbf{r}_\parallel,0)} \mathrm{d}z \int_0^{u_z(\mathbf{r}'_\parallel,0)} \mathrm{d}z' \mathrm{e}^{\mathrm{i}(q_z z - q_z^* z')} \right\rangle \right], \quad (47)\end{aligned}$$

where ρ_{sub} is the average liquid bulk electron density. Neglecting coupling between capillary waves and bulk fluctuations (see below), which amounts to setting the upper integration limit in the first integrals in equation (47) to 0, one can independently calculate the corresponding scattering cross sections.

For Gaussian fluctuations the last integral in equation (47) is equal to $\exp(1/2 \left\langle [u_z(\mathbf{r}_\parallel,0) - u_z(\mathbf{r}'_\parallel,0)]^2 \right\rangle)/\left|q_z^2\right|$ which can be easily calculated using equation (31). The capillary wave scattering cross-section can be written to a good approximation [12,28,29] as:

$$\begin{aligned}\mathrm{d}\sigma/\mathrm{d}\Omega = {} & A r_e^2 \rho^2 \left|t_{0,1}^{\mathrm{in}}\right|^2 \left|t_{0,1}^{\mathrm{sc}}\right|^2 (\widehat{\mathbf{e}}_{\mathrm{in}}.\widehat{\mathbf{e}}_{\mathrm{sc}})^2 \\ & \times \frac{k_B T}{\gamma q_\parallel^2} \left(\frac{q_\parallel}{q_{\max}}\right)^{(k_B T/2\pi\gamma) q_z^2}, \quad (48)\end{aligned}$$

where A is the illuminated area, $q_{\min} = \sqrt{\Delta\rho g/\gamma}$ is the minimum wave vector in the capillary wave spectrum, and $q_{\max}$ is the largest one, on the order $2\pi/$ molecular size.

For density fluctuations,

$$\begin{aligned}\mathrm{d}\sigma/\mathrm{d}\Omega = {} & A r_e^2 \left|t_{0,1}^{\mathrm{in}}\right|^2 \left|t_{0,1}^{\mathrm{sc}}\right|^2 (\widehat{\mathbf{e}}_{\mathrm{in}}.\widehat{\mathbf{e}}_{\mathrm{sc}})^2 \\ & \times \int_{-\infty}^{0} \mathrm{d}z \int_{-\infty}^{0} \mathrm{d}z' \mathrm{e}^{\mathrm{i}q_{z,\mathrm{sub}} z} \mathrm{e}^{-\mathrm{i}q_{z,\mathrm{sub}}^* z'} \\ & \times \int \mathrm{d}\mathbf{r}_\parallel C_{\rho\rho}(\mathbf{r}_\parallel, \mathbf{0}, z, z'; t=0) \mathrm{e}^{\mathrm{i}\mathbf{q}_\parallel \cdot \mathbf{r}_\parallel}, \quad (49)\end{aligned}$$

where $\mathbf{q}_{z,\mathrm{sub}}$ is the normal component of the wave-vector transfer in the liquid. The integration using equation (40) yields:

$$\mathrm{d}\sigma/\mathrm{d}\Omega = A r_e^2 \left|t_{0,1}^{\mathrm{in}}\right|^2 \left|t_{0,1}^{\mathrm{sc}}\right|^2 (\widehat{\mathbf{e}}_{\mathrm{in}} \cdot \widehat{\mathbf{e}}_{\mathrm{sc}})^2 \rho_{\mathrm{sub}}^2 \frac{k_B T\, \kappa_T}{2\ \mathrm{Im}(q_{z,\mathrm{sub}})} . \quad (50)$$

$2\mathrm{Im}(q_{z,\mathrm{sub}})$ is the effective penetration length in the liquid. Quite surprisingly, the result is exactly what one would obtain using the bulk spectrum. It will however be shown in the next section that the frequency dependence of the spectra critically depends on the depth.

Finally, for a liquid, the total scattering due to surface and bulk fluctuations is:

$$\begin{aligned}\mathrm{d}\sigma/\mathrm{d}\Omega = {} & A \rho_{\mathrm{sub}}^2 r_e^2 \left|t_{0,1}^{\mathrm{in}}\right|^2 \left|t_{0,1}^{\mathrm{sc}}\right|^2 (\widehat{\mathbf{e}}_{\mathrm{in}}.\widehat{\mathbf{e}}_{\mathrm{sc}})^2 \\ & \times \left[\frac{k_B T}{\gamma q_\parallel^2} \left(\frac{q_\parallel}{q_{\max}}\right)^{(k_B T/2\pi\gamma) q_z^2} + \frac{k_B T\ \kappa_T}{2\mathrm{Im}(q_{z,\mathrm{sub}})} \right] . \quad (51)\end{aligned}$$

We now come back to the coupling between density fluctuations and capillary waves. In order to estimate its contribution to the scattering, we consider the q component of the thermally induced capillary spectrum on a liquid surface of area $L \times L$. Its average amplitude given by equation (31) is $\zeta = \sqrt{k_B T/\gamma}/(q_\parallel L)$. Half a sinusoidal period of the wave above the reference plane of the non-fluctuating interface contains on average N molecules. The ratio of the scattering cross-section due to fluctuations δN in this number of molecules to the capillary cross-section is $\langle \delta N^2 \rangle / N^2$ according to equation (43), and can be calculated using equation (41) which yields $\langle \delta N^2 \rangle / N^2 = k_B T \kappa_T / V \approx q^2 \sqrt{\gamma k_B T} \kappa_T$ since $V \approx L\zeta/q_\parallel$. Since the capillary wave scattering cross section is proportional to $\rho^2 L^2 k_B T/(\gamma q_\parallel^2)$ and the density fluctuations cross section is proportional to $\rho^2 L^2 k_B T \kappa_T/(2\mathrm{Im}(q_z))$, the ratio of the intensity scattered by density fluctuations in the capillary wave disturbed region to the intensity scattered by density fluctuations within the penetration depth is $2\ \mathrm{Im}(q_z)\sqrt{k_B T/\gamma} \approx 0.05$ for an effective penetration length of 5 nm, and is therefore negligible.

The X-ray intensity scattered by the air-water interface is displayed in Figure 2. Equation (51) is in good agreement with the experimental data for horizontal wave-vector transfer components $q_\parallel$ smaller than 10^9 m^{-1}. The disagreement for larger wave vectors is due to the effect of long range forces and is discussed in reference [14]. As expected the scattering is dominated by density fluctuations for penetration lengths in the μm range and by surface fluctuations for a penetration length of 6 nm and not too large wave vector transfers. For this penetration length density and surface fluctuations make an equivalent contribution to the scattering cross-section for $q_\parallel \approx 10^9$ m^{-1} due to the $\propto q_\parallel^{-2}$ decrease of the surface contribution.

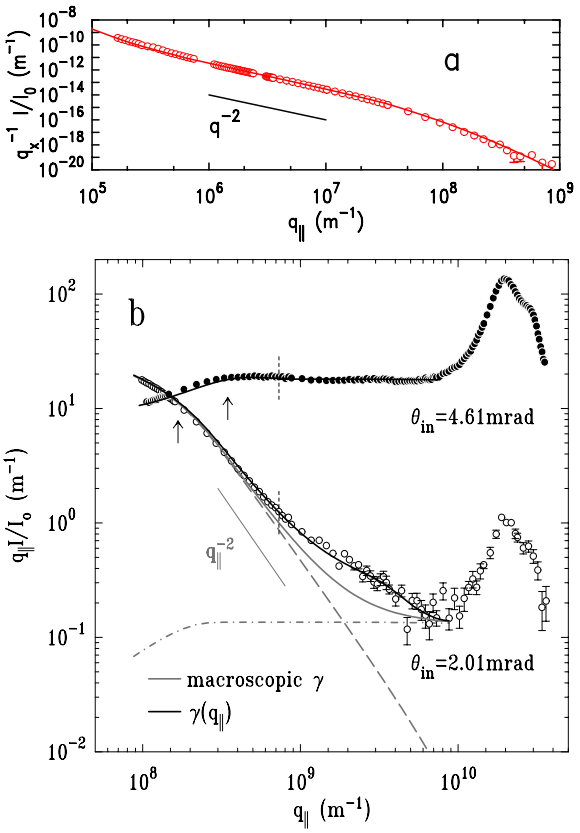

Fig. 2. Scattering at the air-water interface according to reference [14]. (a) Measurements in the plane of incidence (circles) and calculation using equation (48) (line). The data have been divided by $q_\parallel$ to give curves proportional to the scattering cross-section. (b) Scans in the horizontal plane using a vertically mounted PSD (signal integrated between $\theta_{\rm sc} = 10$ mrad and 0.1 rad). The experimental signal has been multiplied by $q_\parallel$ in order to compensate for resolution effects and to obtain curves proportional to the scattering cross-section. Two values of the grazing angle of incidence are shown: $\theta_{in} = 4.61$ mrad ($1/(2\,\mathrm{Im}\,q_{z,\rm sub}) \simeq 10$ μm) and $\theta_{in} = 2.01$ mrad ($1/(2\,\mathrm{Im}\,q_z) \simeq 6$ nm). The continuous grey lines are the result of calculations using equation (51), split into capillary-wave contribution (grey long-dashed line, equation (48) and acoustic-wave contribution (grey short-dashed line, equation (50). The continuous black line has been calculated using a scale-dependent surface energy $\gamma(q_\parallel)$ given by a recent density functional theory [35]. There is no adjustable parameter in any of those calculations. Note the peak at $q_\parallel \approx 2 \times 10^{10}$ m^{-1} giving the short-range structure of nearest neighbours in water. Equation (51) fails for $q_\parallel > 10^9$ m^{-1} where the scale-dependent surface energy must be taken into account.

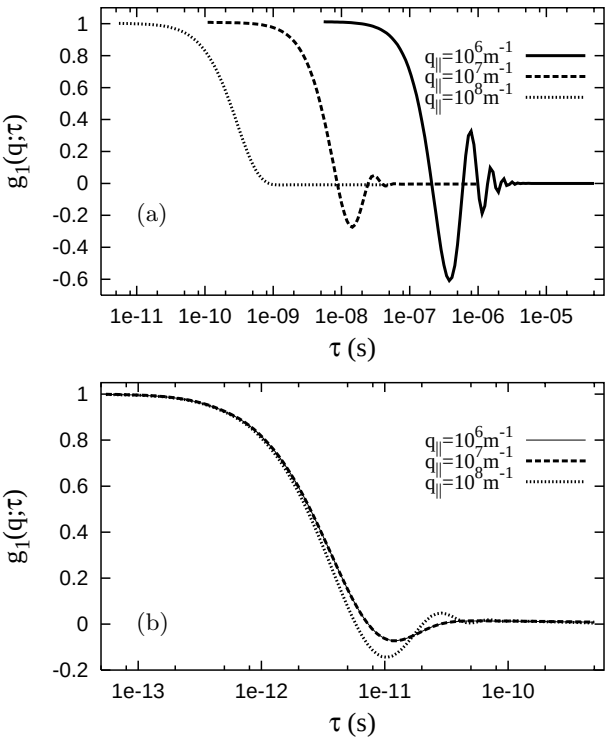

Fig. 3. (a) Surface contribution to $g_1(q,\tau)$ for $q_\parallel = 10^6$, 10^7 and 10^8 m^{-1}: $g_1(q,\tau) = C_{zz}(\mathbf{q},0,0;\tau)/C_{zz}(\mathbf{q},0,0;0)$. (b) Density contribution to $g_1(q,\tau)$ for $q_\parallel = 10^6, 10^7$ and 10^8 m^{-1}: $g_1(q,\tau) = S(q;\tau)/S(q;0)$.

5.3 X-ray photon correlation spectroscopy

The correlation functions we have determined allow us to calculate the time response of the system. Interface dynamics has been widely studied in the micron range using laser light scattering and the interest is now focused on smaller length scales which can in principle be investigated using X-rays. The quantity measured in an X-ray photon correlation spectroscopy experiment is [15]

$$g_2(\mathbf{q},\tau) = \frac{\langle I(t)I(t+\tau)\rangle}{\langle I(t)^2\rangle}\,. \tag{52}$$

For Gaussian fluctuations like the height and density fluctuations we have [30,31],

$$g_2(\mathbf{q},\tau) = 1 + |g_1(\mathbf{q},\tau)|^2, \tag{53}$$

where

$$g_1(\mathbf{q},\tau) = \frac{\langle E(t)E(t+\tau)\rangle}{\langle E(t)^2\rangle}\,. \tag{54}$$

Apart from possible transverse coherence problems [32], equations (45, 49) remain valid, except the correlation functions have now to be calculated for two different times (we need to know the correlations between fluctuations at different points and times). One obtains

See equation (55) next page.

Considering only small q_z values and developing the exponential, we have:

See equation (56) next page.

We now discuss the behavior of g_1 by examining first the surface and density contributions independently. The surface g_1 is plotted in Figure 3a for $\mathbf{q}_\parallel = 10^6$, 10^7, and 10^8 m^{-1}. One can clearly see that the capillary waves are

$$g_1(\mathbf{q},\tau)=\frac{\int \mathrm{d}\mathbf{r}\mathrm{e}^{\mathrm{i}\mathbf{q}_\parallel\cdot\mathbf{r}_\parallel}\left[\frac{\rho_{\mathrm{sub}}^2}{q_z^2}\mathrm{e}^{-\frac{1}{2}q_z^2\langle(u_z(\mathbf{r}_\parallel,0,\tau)-u_z(\mathbf{0},0,0))^2\rangle}+\int_{-\infty}^0\mathrm{d}z\int_{-\infty}^0\mathrm{d}z'\,\mathrm{e}^{\mathrm{i}q_{z,\mathrm{sub}}z}\mathrm{e}^{-\mathrm{i}q_{z,\mathrm{sub}}^*z'}C_{\rho\rho}(\mathbf{q}_\parallel,z,z';\tau)\right]}{\int \mathrm{d}\mathbf{r}_\parallel\mathrm{e}^{\mathrm{i}\mathbf{q}_\parallel\cdot\mathbf{r}_\parallel}\left[\frac{\rho_{\mathrm{sub}}^2}{q_z^2}\mathrm{e}^{-\frac{1}{2}q_z^2\langle(u_z(\mathbf{r}_\parallel,0,0)-u_z(\mathbf{0},0,0))^2\rangle}+\int_{-\infty}^0\mathrm{d}z\int_{-\infty}^0\mathrm{d}z'\,\mathrm{e}^{\mathrm{i}q_{z,\mathrm{sub}}z}\mathrm{e}^{-\mathrm{i}q_{z,\mathrm{sub}}^*z'}C_{\rho\rho}(\mathbf{q}_\parallel,z,z';0)\right]}. \quad (55)$$

$$g_1(\mathbf{q}_\parallel,\tau)=\frac{\int \mathrm{d}\mathbf{r}_\parallel\mathrm{e}^{\mathrm{i}\mathbf{q}_\parallel\cdot\mathbf{r}_\parallel}\left[\rho_{\mathrm{sub}}^2\langle u_z(\mathbf{r}_\parallel,0,\tau)u_z(\mathbf{0},0,0)\rangle+\int_{-\infty}^0\mathrm{d}z\int_{-\infty}^0\mathrm{d}z'\,\mathrm{e}^{\mathrm{i}q_{z,\mathrm{sub}}z}\mathrm{e}^{-\mathrm{i}q_{z,\mathrm{sub}}^*z'}C_{\rho\rho}(\mathbf{q}_\parallel,z,z';\tau)\right]}{\int \mathrm{d}\mathbf{r}_\parallel\mathrm{e}^{\mathrm{i}\mathbf{q}_\parallel\cdot\mathbf{r}_\parallel}\left[\rho_{\mathrm{sub}}^2\langle u_z(\mathbf{r}_\parallel,0,0)u_z(\mathbf{0},0,0)\rangle+\int_{-\infty}^0\mathrm{d}z\int_{-\infty}^0\mathrm{d}z'\,\mathrm{e}^{\mathrm{i}q_{z,\mathrm{sub}}z}\mathrm{e}^{-\mathrm{i}q_{z,\mathrm{sub}}^*z'}C_{\rho\rho}(\mathbf{q}_\parallel,z,z';0)\right]}. \quad (56)$$

propagating for $\mathbf{q}_\parallel = 10^6$ m^{-1}, but that they are damped for $\mathbf{q}_\parallel = 10^8$ m^{-1}.

In contrast to the surface contribution, the density fluctuations contribution (Fig. 3b) does not change very much with the wave vector. This is quite surprising since the acoustic frequencies are quite different for those wave vectors. In order to investigate this point in more detail, we consider

$$S(\mathbf{q};\omega)=\int_{-\infty}^0\mathrm{d}z\int_{-\infty}^0\mathrm{d}z'\times\mathrm{e}^{\mathrm{i}q_{z,\mathrm{sub}}z}\mathrm{e}^{-\mathrm{i}q_{z,\mathrm{sub}}^*z'}C_{\rho\rho}(\mathbf{q}_\parallel,z,z';\omega) \quad (57)$$

which is the time Fourier transform of the density fluctuation contribution to g_1. $S(\mathbf{q};\omega)$ is plotted in Figure 4a for different wavevectors for a penetration depth of 3.1 nm corresponding to standard grazing-incidence experiments. As we can see, there is no peak at the acoustic wave frequency, but a maximum at higher frequencies, which does not seem to depend on the wave vector. The shift from this near-surface behavior to the bulk behavior upon increasing of the penetration depth is displayed in Figure 4b. In order to understand the absence of peak at the acoustic wave frequency, the contribution of the bulk acoustic wave contribution (that in $q_a^z|z-z'|$ in Eq. (36)), of the surface acoustic wave contribution (that in $q_a^z(z+z')$ in Eq. (36)), their sum and the total $S(\mathbf{q};\omega)$ have been plotted together in Figure 4c. It appears that the spectrum in this frequency range is mainly determined by acoustic waves as expected, but that the peak is suppressed by interferences at the surface.

In fact, both the height and density fluctuations contribute to the scattering (Fig. 5a). As expected, surface fluctuations dominate for wave vectors smaller than 10^9 m^{-1}, but this is no longer the case for larger wave vectors. The response function is then determined by a mixing of surface and density fluctuations (Fig. 5b).

We finally briefly examine the possibility of using inelastic X-ray scattering to probe the short scale dynamics of liquid surfaces. This technique has been recently developed as a tool to study fast small-scale dynamics in liquids and solids with energy resolution in the meV range, and has been in particular successfully applied to the investigation of high frequency dynamics of liquid water [17,33,34]. These experiments have in particular shown that hydrodynamics models were valid up to wave vectors as large

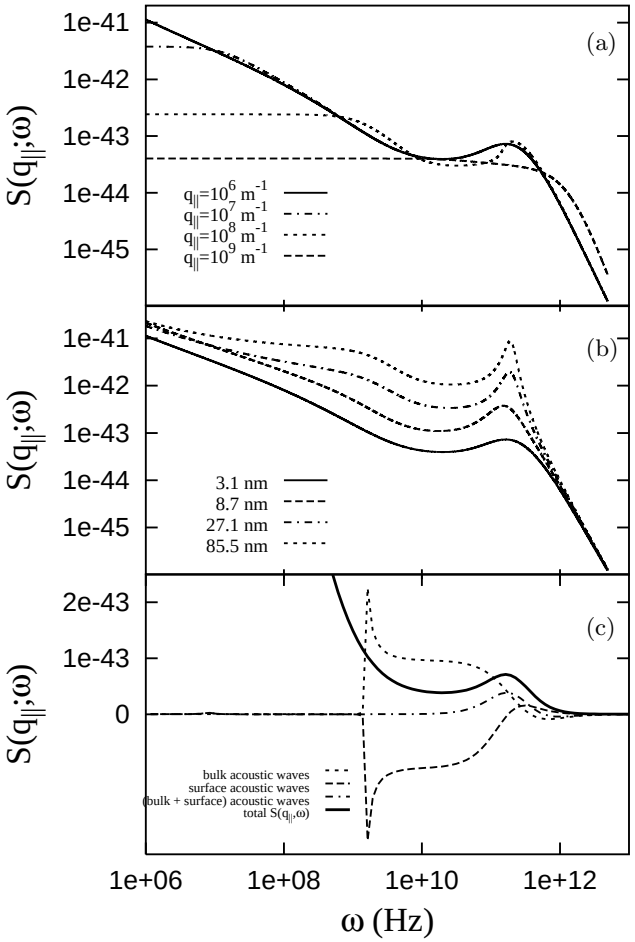

Fig. 4. (a) Surface density correlation function integrated over 3.1 nm corresponding to the effective penetration depth in a standard grazing incidence X-ray scattering experiment for $q_\parallel = 10^6$ m^{-1}, 10^7 m^{-1}, 10^8 m^{-1}, and 10^9 m^{-1} respectively. There is no peak at the acoustic wave frequency, but a maximum at higher frequencies. (b) Surface density correlation function integrated over 3.1 nm, 8.7 nm, 27.1 nm and 85.5 nm respectively for an in-plane wave vector $q_\parallel = 10^6$ m^{-1}. Note how the acoustic wave peak is restored with increasing penetration depth. (c) Surface density correlation function integrated over 3.1 nm, for a wave vector $q_\parallel = 10^6$ m^{-1}. Bulk acoustic wave contribution, surface acoustic wave contribution, sum of them, and total $S(\mathbf{q},\omega)$. Interferences at the surface suppress the peak at the acoustic wave frequency.

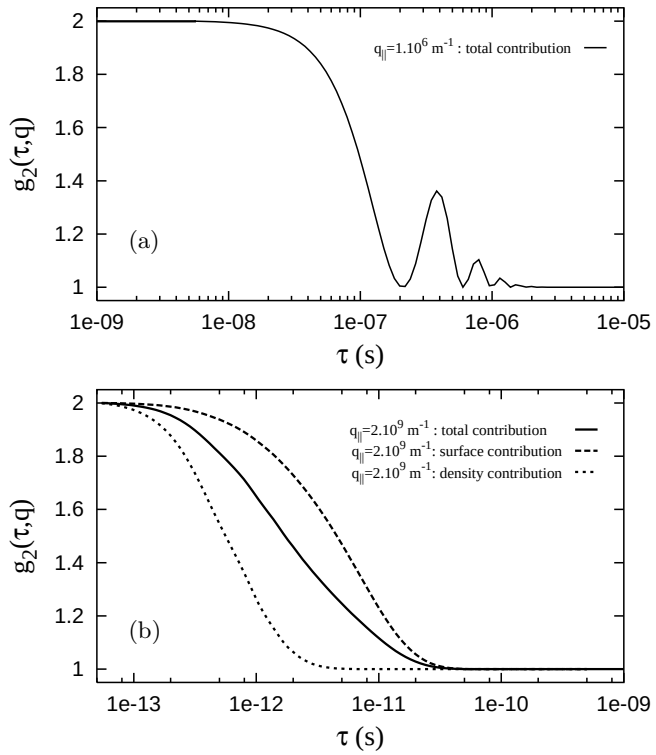

Fig. 5. (a) $g_2(\mathbf{q},\tau)$ for $q_\parallel = 10^6$ m^{-1}. g_2 only depends on surface properties since bulk contribution is perfectly negligible. (b) $g_2(\mathbf{q},\tau)$ for $q_\parallel = 2\times10^9$ m^{-1}: bulk contribution is no longer negligible.

as 2×10^9 m^{-1}, supporting the validity of our calculations down to the nanometer scale. The scattering cross-section for inelastic scattering is:

$$\frac{\mathrm{d}^2\sigma}{\mathrm{d}\Omega\mathrm{d}\omega} = r_e^2 \left|t_{0,1}^{\mathrm{in}}\right|^2 \left|t_{0,1}^{\mathrm{sc}}\right|^2 (\widehat{\mathbf{e}}_{\mathrm{in}}.\widehat{\mathbf{e}}_{\mathrm{sc}})^2 \times \left\langle \left| \int \mathrm{d}\mathbf{r}\mathrm{d}\mathbf{r}' \delta\rho_e(\mathbf{r},\tau)\delta\rho_e(\mathbf{r}',0) \mathrm{e}^{\mathrm{i}\mathbf{q}.(\mathbf{r}-\mathbf{r}')} \mathrm{e}^{\mathrm{i}\omega\tau} \right|^2 \right\rangle, \quad (58)$$

leading in our case to:

$$\frac{\mathrm{d}^2\sigma}{\mathrm{d}\Omega\mathrm{d}\omega} = r_e^2 \left|t_{0,1}^{\mathrm{in}}\right|^2 \left|t_{0,1}^{\mathrm{sc}}\right|^2 (\widehat{\mathbf{e}}_{\mathrm{in}}.\widehat{\mathbf{e}}_{\mathrm{sc}})^2 \left[\rho_{\mathrm{sub}}^2 C_{zz}(\mathbf{q}_\parallel,0,\omega) + \int_{-\infty}^{0}\mathrm{d}z \int_{-\infty}^{0}\mathrm{d}z'\, \mathrm{e}^{\mathrm{i}q_{z,\mathrm{sub}}z} \mathrm{e}^{-\mathrm{i}q_{z,\mathrm{sub}}^{*}z'} C_{\rho\rho}(\mathbf{q}_\parallel,z,z';\omega)\right], \quad (59)$$

where the first term is the height fluctuation contribution and the second term the density fluctuation contribution. Density fluctuations have been measured in the bulk. We can use equation (59) to evaluate their contribution at the surface which should be in the ratio of the scattering volume heights which are equal to the penetration length in the surface case and to the entrance slit height in the bulk experiment. This ratio is equal to $(1/2\mathrm{Im}q_z)/100\ \mu\mathrm{m} \approx 10^{-4}$ and such experiments would therefore be extremely difficult. On the other hand, the detection of capillary waves should be limited by the energy resolution.

Concluding remarks

Our calculations provide a firm basis for X-ray scattering experiments of the liquid surface. They show in particular that density fluctuations cannot be neglected in general. We have also derived complete expressions for the interpretation of X-ray photon correlation spectroscopy experiments for the first time. Such experiments should be the best way to investigate the short-scale dynamics of liquid surfaces, and more experiments are now needed to improve our understanding. In particular, the correlation functions we obtain are far from the simple exponentials assumed in reference [15]. In any quantitative analysis, it will also be important to consider that real sources are only partially coherent.

References

1. J.S. Rowlinson, B. Widom, *Molecular theory of capillarity*, in *The international series of monographs on chemistry.* Vol. 8 (Oxford University Press, Oxford, 1982)
2. R.H. Katyl, U. Ingard, Phys. Rev. Lett. **19**, 64 (1967)
3. R.H. Katyl, U. Ingard, Phys. Rev. Lett. **20**, 248 (1968)
4. M.A. Bouchiat, J. Meunier, C.R. Acad. Sc. Paris, Série B **266**, 301 (1968)
5. D. Langevin, J. Chem. Soc. Faraday Trans. I **70**, 95 (1974)
6. S. Hard *et al.*, J. Appl. Phys. **47**, 2433 (1976)
7. D. Byrne, J.C. Earnshaw, J. Phys. D **10**, L207 (1977)
8. M.A Bouchiat, D. Langevin, J. Colloid Interface Sci. **63**, 193 (1978)
9. J.C. Earnshaw, Nature **192**, 138 (1981)
10. A. Braslau, M. Deutsch, P.S. Pershan, A.H. Weiss, J. Als-Nielsen, J. Bohr, Phys. Rev. Lett. **54**, 114 (1985)
11. D.K. Schwartz, M.L. Schlossman, E.H. Kawamoto, G.J. Kellogg, P.S. Pershan, B.M. Ocko, Phys. Rev. A **41**, 5687 (1990)
12. M.K. Sanyal, S.K. Sinha, K.G. Huang, B.M. Ocko, Phys. Rev. Lett. **66**, 628 (1991)
13. J. Daillant, O. Bélorgey, J. Chem. Phys. **97**, 5837 (1992)
14. C. Fradin, A. Braslau, D. Luzet, D. Smilgies, M. Alba, N. Boudet, K. Mecke, J. Daillant, Nature **403**, 871 (2000)
15. T. Seydel, A. Madsen, M. Tolan, G. Grübel, W. Press, Phys. Rev. B **63**, 3409 (2001)
16. R. Loudon, *Ripples on liquid interfaces*, *Surface excitations*, Vol. 9 of *Modern problems in condensed matter sciences*, edited by V.M. Agranovich, R. Loudon (North-Holland Physics Publishing, Amsterdam, 1984), pp. 589–638
17. G. Ruocco, F. Sette, J. Phys. Cond. Matt. **11**, 259 (1999)
18. M.G. Cottam, A.A. Maradudin, *Surface excitations*, Vol. 9 of *Modern problems in condensed matter sciences*, edited by V.M. Agranovich, R. Loudon (North-Holland Physics Publishing, Amsterdam, 1984)
19. L.P. Kadanoff, P.C. Martin, Ann. Phys. **24**, 419 (1963)
20. L.E. Reichl, *A Modern Course in Statistical Physics* (Edward Arnold, 1980)

21. R. Loudon, Proc. R. Soc. Lond. **372**, 275 (1980)
22. T.A. Litovitz, E.H. Carnevale, J. Appl. Phys. **26**, 816 (1955)
23. R. Loudon, J. Raman Spectroscopy **7**, 10 (1978)
24. U.-S. Jeng, L. Esibov, L. Crow, A. Steyerl, J. Phys. Cond. Matt. **10**, 4955 (1998)
25. L.D. Landau, E.M. Lifshitz, *Electrodynamics of continuous media*, Vol. 8 of *Course of theoretical physics* (Pergamon Press, Oxford, 1960)
26. J. Daillant, A. Sentenac, *Diffuse scattering, X-ray and neutron reflectivity: principles and applications*, Vol. 58 of *Lecture notes in physics*, edited by J. Daillant, A. Gibaud (Heidelberg, Springer-Verlag, 1999), pp. 121–162
27. J. Daillant, M. Alba, Rep. Prog. Phys. **63**, 1725 (2000)
28. S.K. Sinha, E.B. Sirota, S. Garoff, Phys. Rev. B **38**, 2297 (1988)
29. M. Fukuto, R.K. Heilmann, P.S. Pershan, J.A. Griffiths, S.M. Yu, D.A. Tirrel, Phys. Rev. Lett. **81**, 3455 (1998)
30. B.J Berne, R. Pecora, *Dynamic light scattering* (Wiley-Interscience, 1975)
31. B. Chu, *Laser light scattering*, (Academic Press, 1991)
32. S.K. Sinha, M. Tolan, A. Gibaud, Phys. Rev. B **57**, 2740 (1998)
33. F. Sette, G. Ruocco, U. Bergmann, C. Masciovecchio, G. Signorelli, R. Verbeni, Phys. Rev. Lett. **75**, 850 (1995)
34. G. Monaco, A. Cunsolo, G. Ruocco, F. Sette, Phys. Rev. E **60**, 5505 (1999)
35. K.R. Mecke, S. Dietrich, Phys. Rev. E **59**, 6766 (1999)